

Iterative Overlap QRM-MLBD for Single-Carrier MIMO Transmission Without CP Insertion

Hideyuki MOROGA¹ Tetsuya YAMAMOTO¹ and Fumiyuki ADACHI²

^{1,2}Dept. of Electrical and Communication Engineering, Graduate School of Engineering, Tohoku University
6-6-05 Aza-Aoba, Aramaki, Aoba-ku, Sendai, 980-8579 Japan

¹{moroga, yamamoto}@mobile.ecei.tohoku.ac.jp, ²adachi@ecei.tohoku.ac.jp

Abstract—QR decomposition and M-algorithm based near maximum likelihood block detection (QRM-MLBD) is a computationally efficient near ML detection scheme. It can significantly improve the transmission performance of the single-carrier (SC) multi-input multi-output (MIMO) transmissions in a frequency-selective fading channel compared to the conventional minimum mean square error (MMSE) based linear detection. In the conventional QRM-MLBD, the insertion of the cyclic prefix (CP) is necessary in order to avoid inter-block interference (IBI). However, the CP insertion reduces the transmission efficiency. In this paper, we propose an overlap QRM-MLBD which requires no CP insertion. We evaluate the throughput performance by computer simulation to compare it with the conventional QRM-MLBD with CP insertion.

Keywords—component; Single-carrier, MIMO, no cyclic prefix, QR decomposition, M-algorithm

I. INTRODUCTION

Multi-input multi-output (MIMO) spatial multiplexing [1] achieves high data rate transmissions without increasing the signal bandwidth. Single-carrier (SC) transmission is suitable for the uplink applications because of its lower peak-to-average power ratio (PAPR) property [2, 3] compared to multi-carrier transmission, e.g., orthogonal frequency division multiplexing (OFDM) [4]. SC-MIMO has been adopted for uplink transmissions of 3rd generation partnership project long term evolution (3GPP LTE) systems [5].

The wireless channel is severely frequency-selective for the broadband signal transmissions [6]. SC-MIMO spatial multiplexing suffers from inter-symbol interference (ISI) arising from the severe frequency-selectivity of the channel. The use of the cyclic prefix (CP) and frequency-domain block detection such as a computationally efficient minimum mean square error (MMSE) based linear detection [7] can improve the transmission performance of SC-MIMO spatial multiplexing. However, a big performance gap from the maximum likelihood (ML) performance still exists due to the presence of residual ISI and inter-antenna interference (IAI). Recently, QR decomposition and M-algorithm based near maximum likelihood block detection (QRM-MLBD) [8, 9] was proposed for broadband SC-MIMO transmission. It was shown that QRM-MLBD significantly improves the transmission performance of SC-MIMO spatial multiplexing in a frequency-selective fading channel with significantly lower computational complexity compared to full ML detection.

The conventional block detection schemes, such as linear MMSE detection and QRM-MLBD require the insertion of CP

to avoid the inter-block interference (IBI). However, the CP insertion reduces the transmission efficiency. In case of linear detection, overlap frequency-domain linear detection was proposed [10-12]. However, a big performance gap from the ML performance exists due to the insufficient suppression of interferences, i.e., IAI, ISI, and IBI.

In this paper, we propose an overlap QRM-MLBD for SC-MIMO system without CP insertion. The joint use of overlap processing and QRM-MLBD is expected to achieve the near ML performance. Recently, we have presented the SC transmission using overlap QRM-MLBD in [13, 14], which requires no CP insertion and provides close-to-ML performance for single-input single-output (SISO) systems. To extend our previously proposed overlap QRM-MLBD to the MIMO systems, we introduce an appropriate modification of the received signal vector for SC-MIMO transmission.

The rest of the paper is organized as follows. Section II presents the overlap QRM-MLBD. In Section III, we present the simulation results. The throughput performance achievable with overlap QRM-MLBD is compared with the conventional QRM-MLBD with CP insertion. The computational complexity of the proposed overlap QRM-MLBD is also discussed. Finally, in Section IV, we conclude the paper.

II. OVERLAP QRM-MLBD

A. Transmission System

Figure 1 illustrates the system model of SC-MIMO with the overlap QRM-MLBD. Figure 2 shows block signal processing of overlap QRM-MLBD. At the transmitter, the data-modulated symbol sequence is serial-to-parallel (S/P) converted to N_t parallel symbol sequences, each to be transmitted from a different transmit antenna.

At the receiver, the received signal of each received antenna is divided into a sequence of blocks of X symbols to be picked up (called X -symbol block). The received signal vector at the n_r -th receive antenna $\mathbf{y}_{n_r} = [y_{n_r}(0), \dots, y_{n_r}(t), \dots, y_{n_r}(N_c + L - 2)]^T$ of $N_c + L - 1$ symbols (called observation window) is stored to detect a block of N_c symbols including X -symbol block at the beginning for each transmit antenna, where L is the number of propagation paths. In the i -th iteration stage, the replica of IBI from the previous block is generated by using the i -th stage decision of previous block. The replica of IBI from the next block is generated by the $(i-1)$ -th stage decision of next block. The IBIs are removed by subtracting its replicas from the received signal sequence over the observation window before applying QRM-MLBD. After modification of the received

signal vector and QRM-MLBD, the first X -symbol block is picked up for each transmit antenna. To detect the next X -symbol block, the observation window is shifted by X -symbol block as shown in Fig. 2. By repeating this process, the continuously transmitted symbol sequence can be detected. This process is iteratively performed I times ($I=0$ represents the initial detection) to suppress residual IBI.

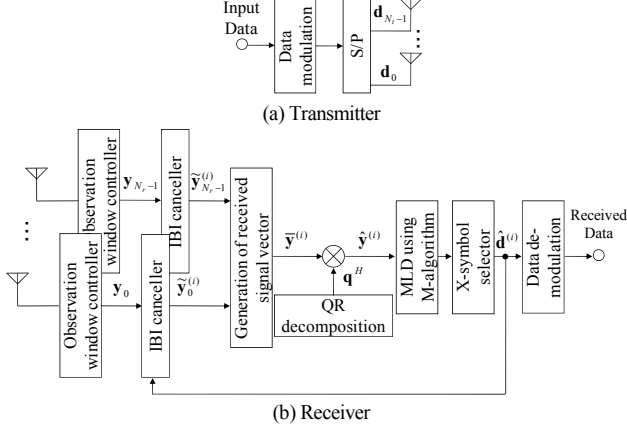


Figure 1. System model.

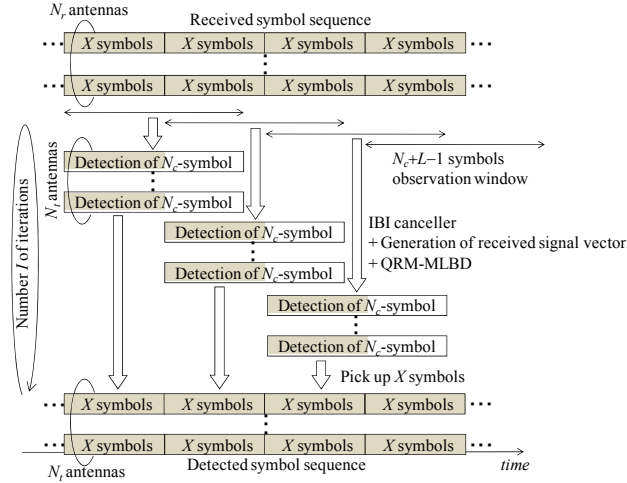


Figure 2. Overlap QRM-MLBD.

B. Received Signal Representation

We assume a symbol-spaced frequency-selective fading channel composed of L propagation paths with different time delays. The channel impulse response between the n_r -th transmit antenna and the n_r -th receive antenna $h_{n_r,n_r}(\tau)$ is given by

$$h_{n_r,n_r}(\tau) = \sum_{l=0}^{L-1} h_{n_r,n_r,l} \delta(\tau - \tau_l), \quad (1)$$

where $h_{n_r,n_r,l}$ and τ_l are respectively the complex-valued path gain with $E[\sum_{l=0}^{L-1} |h_{n_r,n_r,l}|^2] = 1$ and the time delay of the l -th path. The received signal sequence at the n_r -th receive antenna $\mathbf{y}_{n_r} = [y_{n_r}(0), \dots, y_{n_r}(t), \dots, y_{n_r}(N_c + L - 2)]^T$ of $N_c + L - 1$ symbols

over the observation window can be expressed using the matrix form as

$$\mathbf{y}_{n_r} = \sqrt{\frac{2E_s}{T_s N_t}} \sum_{n_t=0}^{N_t-1} \mathbf{H}_{n_r,n_t} \mathbf{d}_{n_t} + \sqrt{\frac{2E_s}{T_s N_t}} \sum_{n_t=0}^{N_t-1} \mathbf{H}_{n_r,n_t,-1} \mathbf{d}_{n_t,-1} + \sqrt{\frac{2E_s}{T_s N_t}} \sum_{n_t=0}^{N_t-1} \mathbf{H}_{n_r,n_t,+1} \mathbf{d}_{n_t,+1} + \mathbf{n}_{n_r}, \quad (2)$$

where E_s and T_s are respectively the symbol energy and duration. $\mathbf{d}_{n_t} = [d_{n_t}(0), \dots, d_{n_t}(t), \dots, d_{n_t}(N_c - 1)]^T$ represents the desired transmit symbol sequence of the n_t -th transmit antenna. $\mathbf{d}_{n_t,-1} = [d_{n_t,-1}(0), \dots, d_{n_t,-1}(t), \dots, d_{n_t,-1}(N_c - 1)]^T$ and $\mathbf{d}_{n_t,+1} = [d_{n_t,+1}(0), \dots, d_{n_t,+1}(t), \dots, d_{n_t,+1}(N_c - 1)]^T$ represent the transmit symbol sequences in the previous block and in the next block, respectively. The first term of Eq. (2) represents the desired signal component. The second and the third terms represent the IBI components from the previous block and from the next block, respectively. $\mathbf{n}_{n_r} = [n_{n_r}(0), \dots, n_{n_r}(t), \dots, n_{n_r}(N_c + L - 2)]^T$ is the noise vector. The t -th element, $n_{n_r}(t)$, of \mathbf{n}_{n_r} is the zero-mean complex Gaussian variable having the variance $2N_0/T_s$ with N_0 being the one-sided power spectrum density of the additive white Gaussian noise (AWGN). \mathbf{H}_{n_r,n_t} , $\mathbf{H}_{n_r,n_t,-1}$, and $\mathbf{H}_{n_r,n_t,+1}$ are respectively $(N_c + L - 1) \times N_c$ channel impulse response matrixes between the n_t -th transmit antenna and n_r -th receive antenna, given as

$$\mathbf{H}_{n_r,n_t} = \begin{bmatrix} h_{n_r,n_t,0} & & & \mathbf{0} \\ \vdots & \ddots & & \\ h_{n_r,n_t,L-1} & & \ddots & h_{n_r,n_t,0} \\ \mathbf{0} & & & h_{n_r,n_t,L-1} \end{bmatrix}$$

$$\mathbf{H}_{n_r,n_t,-1} = \begin{bmatrix} h_{n_r,n_t,L-1} & \dots & h_{n_r,n_t,1} \\ \vdots & \ddots & \vdots \\ \mathbf{0} & & h_{n_r,n_t,L-1} \end{bmatrix}$$

$$\mathbf{H}_{n_r,n_t,+1} = \begin{bmatrix} & & & \mathbf{0} \\ & & & \\ h_{n_r,n_t,0} & \dots & h_{n_r,n_t,L-2} \\ \vdots & \ddots & \vdots \end{bmatrix}. \quad (3)$$

C. Overlap QRM-MLBD

1) Overall received signal vector

In the i -th iteration stage, the IBI replica from the previous block is generated by using the decision of

$\hat{\mathbf{d}}_{n_t-1}^{(i)} = [\hat{d}_{n_t-1}^{(i)}(0), \dots, \hat{d}_{n_t-1}^{(i)}(t), \dots, \hat{d}_{n_t-1}^{(i)}(N_c - 1)]^T$, $n_t=0 \sim N_t-1$, of the previous block. When $t \geq 1$, the IBI replica from the next block is also generated by using the decision of $\hat{\mathbf{d}}_{n_t-1}^{(i-1)} = [\hat{d}_{n_t-1}^{(i-1)}(0), \dots, \hat{d}_{n_t-1}^{(i-1)}(t), \dots, \hat{d}_{n_t-1}^{(i-1)}(N_c - 1)]^T$, $n_t=0 \sim N_t-1$, of the next block. The IBI cancellation is performed by subtracting the IBI replicas from the received signal as

$$\tilde{\mathbf{y}}_{n_r}^{(i)} = \mathbf{y}_{n_r} - \begin{pmatrix} \sqrt{\frac{2E_s}{T_s N_t}} \sum_{n=0}^{N_t-1} \mathbf{H}_{n_r, n_t-1} \hat{\mathbf{d}}_{n_t-1}^{(i)} \\ + \sqrt{\frac{2E_s}{T_s N_t}} \sum_{n=0}^{N_t-1} \mathbf{H}_{n_r, n_t+1} \hat{\mathbf{d}}_{n_t+1}^{(i-1)} \end{pmatrix}. \quad (4)$$

The overall received signal vector $\bar{\mathbf{y}}^{(i)}$ is expressed as

$$\begin{aligned} \bar{\mathbf{y}}^{(i)} &= [\{\tilde{\mathbf{y}}_0^{(i)}\}^T \dots \{\tilde{\mathbf{y}}_{N_r-1}^{(i)}\}^T]^T \\ &= \sqrt{\frac{2E_s}{T_s N_t}} \begin{bmatrix} \mathbf{H}_{0,0} & \dots & \mathbf{H}_{0,N_r-1} \\ \vdots & \ddots & \vdots \\ \mathbf{H}_{N_r-1,0} & \dots & \mathbf{H}_{N_r-1,N_r-1} \end{bmatrix} \begin{bmatrix} \mathbf{d}_0 \\ \vdots \\ \mathbf{d}_{N_r-1} \end{bmatrix} + \begin{bmatrix} \mathbf{n}_0 \\ \vdots \\ \mathbf{n}_{N_r-1} \end{bmatrix} \\ &+ \sqrt{\frac{2E_s}{T_s N_t}} \begin{bmatrix} \mathbf{H}_{0,0,-1} & \dots & \mathbf{H}_{0,N_r-1,-1} \\ \vdots & \ddots & \vdots \\ \mathbf{H}_{N_r-1,0,-1} & \dots & \mathbf{H}_{N_r-1,N_r-1,-1} \end{bmatrix} \begin{bmatrix} \mathbf{d}_{0,-1} - \hat{\mathbf{d}}_{0,-1}^{(i)} \\ \vdots \\ \mathbf{d}_{N_r-1,-1} - \hat{\mathbf{d}}_{N_r-1,-1}^{(i)} \end{bmatrix}, \\ &+ \sqrt{\frac{2E_s}{T_s N_t}} \begin{bmatrix} \mathbf{H}_{0,0,+1} & \dots & \mathbf{H}_{0,N_r-1,+1} \\ \vdots & \ddots & \vdots \\ \mathbf{H}_{N_r-1,0,+1} & \dots & \mathbf{H}_{N_r-1,N_r-1,+1} \end{bmatrix} \begin{bmatrix} \mathbf{d}_{0,+1} - \hat{\mathbf{d}}_{0,+1}^{(i-1)} \\ \vdots \\ \mathbf{d}_{N_r-1,+1} - \hat{\mathbf{d}}_{N_r-1,+1}^{(i-1)} \end{bmatrix} \\ &= \sqrt{\frac{2E_s}{T_s N_t}} \bar{\mathbf{H}} \bar{\mathbf{d}} + \sqrt{\frac{2E_s}{T_s N_t}} \bar{\mathbf{H}}_{-1} (\bar{\mathbf{d}}_{-1} - \hat{\mathbf{d}}_{-1}^{(i)}) \\ &+ \sqrt{\frac{2E_s}{T_s N_t}} \bar{\mathbf{H}}_{+1} (\bar{\mathbf{d}}_{+1} - \hat{\mathbf{d}}_{+1}^{(i-1)}) + \bar{\mathbf{n}} \end{aligned} \quad (5)$$

where $\bar{\mathbf{H}}$, $\bar{\mathbf{H}}_{-1}$, and $\bar{\mathbf{H}}_{+1}$ are extended channel matrixes of size $N_r(N_c+L-1) \times N_r N_c$. $\bar{\mathbf{d}}$, $\bar{\mathbf{d}}_{-1}$, and $\bar{\mathbf{d}}_{+1}$ are overall transmit symbol vectors of size $N_r N_c \times 1$. The second and the third terms of Eq. (5) are the residual IBIs from the previous and next blocks, respectively.

2) Modification of the overall received signal vector

Overlap QRM-MLBD for SISO systems [13, 14] utilizes the property that the IBI from the next block, which cannot be removed in the initial iteration stage, exists only on the elements near the bottom of the received signal vector. QRM-MLBD is applied to the received signal vector and then, IBI from the next block is less significant at the symbols closer to the beginning of block. Therefore, symbol error rate near the beginning of block is lower and symbol error rate near the end of block is higher. Based on the above observation, overlap QRM-MLBD can effectively suppress the IBI by picking up only the reliable first X -symbol block from the detected block. However, in Eq. (5), the IBI from the next block exists on the elements near the bottom of each received signal vector. Therefore, if QRM-MLBD is applied to Eq. (5) directly, the effect of IBI spreads over the entire symbols in the block. To

extend the overlap QRM-MLBD to the MIMO systems, we modify the overall received signal vector as

$$\bar{\mathbf{y}}^{(i)} = [\{\tilde{\mathbf{y}}_0^{(i)}(0)\}^T, \dots, \{\tilde{\mathbf{y}}_0^{(i)}(t)\}^T, \dots, \{\tilde{\mathbf{y}}_0^{(i)}(N_c - L - 2)\}^T]^T, \quad (6)$$

where $\tilde{\mathbf{y}}^{(i)}(t) = [\tilde{y}_0^{(i)}(t), \dots, \tilde{y}_{N_r-1}^{(i)}(t)]^T$ denotes the received signal vector after IBI cancellation at t -th symbol of size $N_r \times 1$. After above modification, the extended channel matrixes corresponding to the IBIs from the previous and the next block are permuted as

$$\left\{ \begin{array}{l} \bar{\mathbf{H}}'_{-1} = \begin{bmatrix} \mathbf{h}'_{0,L-1} & \dots & \mathbf{h}'_{0,1} & \mathbf{h}'_{N_r-1,L-1} & \dots & \mathbf{h}'_{N_r-1,1} \\ \vdots & \ddots & \vdots & \vdots & \ddots & \vdots \\ & & \mathbf{h}'_{0,L-1} & & & \mathbf{h}'_{N_r-1,L-1} \\ \mathbf{0} & & & \mathbf{0} & & \\ & & & & & \mathbf{0} \end{bmatrix} \\ \bar{\mathbf{H}}'_{+1} = \begin{bmatrix} & & & & & \\ & & & & & \mathbf{0} \\ & & & & & \mathbf{0} \\ \mathbf{h}'_{0,1} & & & \mathbf{h}'_{N_r-1,0} & & \\ \vdots & \ddots & & \vdots & \ddots & \\ \mathbf{h}'_{0,L-2} & \dots & \mathbf{h}'_{0,0} & \mathbf{h}'_{N_r-1,L-2} & \dots & \mathbf{h}'_{N_r-1,0} \end{bmatrix} \end{array} \right\}, \quad (7)$$

where $\mathbf{h}'_{n_r,l} = [h_{0,n_r,l}, \dots, h_{N_r-1,n_r,l}]^T$. It can be seen from Eqs. (6) and (7) that the IBI from the next block exists only the elements near the bottom of the modified overall received signal vector.

In QRM-MLBD, the M-algorithm [15] is performed starting from the last symbol in the overall transmit symbol vector. Since overlap QRM-MLBD outputs only X -symbol block for each transmit antenna which has less significant effect of the IBI from the next symbol block, the order of $N_r N_c$ symbols in the desired overall transmit symbol vector $\bar{\mathbf{d}}$ is changed as

$$\bar{\mathbf{d}}' = [\mathbf{d}^T(N_c - 1), \dots, \mathbf{d}^T(t), \dots, \mathbf{d}^T(0)]^T, \quad (8)$$

where $\mathbf{d}(t) = [d_0(t), \dots, d_{N_r-1}(t)]^T$ denotes the transmit symbol vector at t -th symbol of size $N_r \times 1$. By doing above modification and ordering, the extended channel matrix for the desired signal component $\bar{\mathbf{H}}$ is given as

$$\bar{\mathbf{H}}'' = \begin{bmatrix} \mathbf{0} & & & & \mathbf{H}''_{L-1} \\ & & & & \vdots \\ & & & & \mathbf{H}''_0 \\ \mathbf{H}''_{L-1} & & & & \\ \vdots & \ddots & & & \\ \mathbf{H}''_0 & & & & \mathbf{0} \end{bmatrix}, \quad (9)$$

where

$$\bar{\mathbf{H}}'' = \begin{bmatrix} h_{0,0,l} & \dots & h_{0,N_r-1,l} \\ \vdots & \ddots & \vdots \\ h_{N_r-1,0,l} & \dots & h_{N_r-1,N_r-1,l} \end{bmatrix}. \quad (10)$$

It can be seen from Eqs. (6), (9), and (10) that the overall received signal vector can be represented similar to the SISO case [14] as shown in Fig. 3. Therefore, previously proposed overlap QRM-MLBD can be developed to the MIMO system.

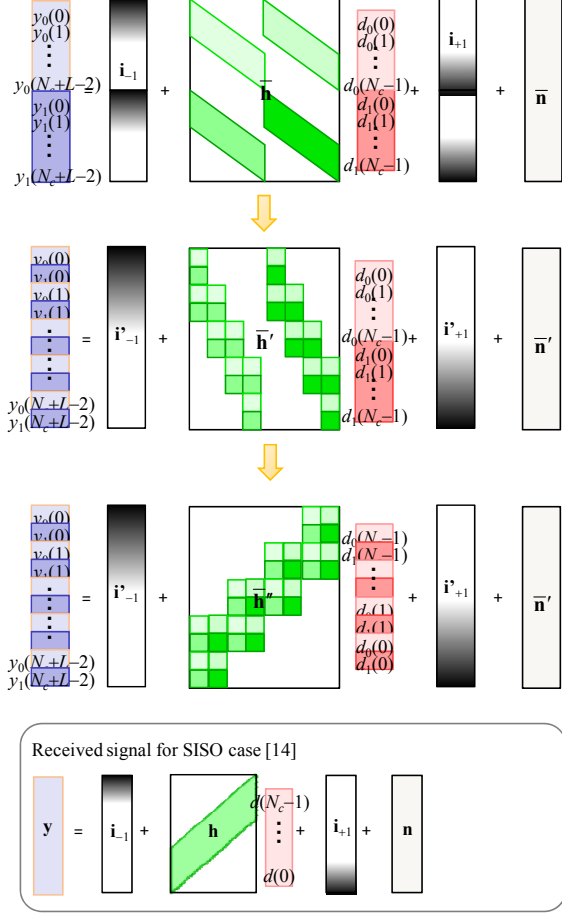


Figure 3. Modification of the overall received signal vector.

3) QRM-MLBD

QR decomposition is applied to $\bar{\mathbf{H}}^n$ as $\bar{\mathbf{H}}^n = \mathbf{Q}\mathbf{R}$ where \mathbf{Q} is an $N_r(N_c+L-1) \times N_r N_c$ unitary matrix satisfying $\mathbf{Q}^H \mathbf{Q} = \mathbf{I}$ (\mathbf{I} is the identity matrix) and \mathbf{R} is an $N_r N_c \times N_r N_c$ upper triangular matrix. $(\cdot)^H$ denotes the Hermitian transpose operation. By left multiplying \mathbf{Q}^H to $\bar{\mathbf{y}}^{(i)}$, we obtain the transformed signal vector given by

$$\begin{aligned} \hat{\mathbf{y}}^{(i)} &= \mathbf{Q}^H \bar{\mathbf{y}}^{(i)} \\ &= \sqrt{\frac{2E_s}{T_s N_t}} \mathbf{R} \mathbf{d}' + \sqrt{\frac{2E_s}{T_s N_t}} \hat{\mathbf{H}}_{-1} (\bar{\mathbf{d}}_{-1} - \hat{\mathbf{d}}_{-1}^{(i)}) \\ &\quad + \sqrt{\frac{2E_s}{T_s N_t}} \hat{\mathbf{H}}_{+1} (\bar{\mathbf{d}}_{+1} - \hat{\mathbf{d}}_{+1}^{(i-1)}) + \hat{\mathbf{n}} \end{aligned} \quad (11)$$

where $\hat{\mathbf{H}}_{-1} = \mathbf{Q}^H \bar{\mathbf{H}}_{-1}$, $\hat{\mathbf{H}}_{+1} = \mathbf{Q}^H \bar{\mathbf{H}}_{+1}$, and $\hat{\mathbf{n}} = \mathbf{Q}^H \bar{\mathbf{n}}$.

From Eq. (11), the ML solution can be obtained by searching for the best path having the minimum Euclidean distance in the tree diagram composed of $N_r N_c$ stages. M-algorithm is used to reduce the detection complexity of the tree search. In each stage, the best M paths are selected as surviving

paths by comparing the path metrics based on the squared Euclidean distance for all surviving paths and are passed to the next stage. The data demodulation is carried out by tracing back the path having the smallest path metric at the last stage. In this paper, the stopping criterion [14] can be applied similar to the SISO case to stop the tree search at an earlier stage to reduce the detection complexity.

III. COMPUTER SIMULATION

The throughput performance of 2×2 SC-MIMO spatial multiplexing using overlap QRM-MLBD is evaluated by computer simulation. The simulation condition is shown in Table I. We consider 16QAM data modulation, packet size $N_p=192$, and CP length $N_g=0$. The channel is assumed to be a frequency-selective block Rayleigh fading channel having $L=16$ -path uniform power delay profile. We assume that there is no fading variation in one packet and ideal channel estimation is assumed.

TABLE I. COMPUTER SIMULATION CONDITION

		16QAM
Transmitter	Modulation	16QAM
	Number of transmit antennas	$N_t=2$
	Packet size	$N_p=192$ symbols
	GI length	$N_g=16$
Channel	Fading type	Frequency-selective block Rayleigh
	Power delay profile	$L=16$ -path uniform
	Time delay	$\tau=l$ ($l=0-L-1$)
Receiver	Number of receive antennas	$N_r=2$
	Channel estimation	Ideal

A. Throughput Performance

Figure 4 plots the throughput performance as a function of average received E_s/N_0 with X as a parameter for $N_c=64$, $I=0, 1$, $M=16$. In this paper, the throughput is defined as $N \log_2 Z \times (1-\text{PER}) / (1+N_g/N_c)$, where Z is the modulation level and PER denotes the packet error rate. The throughput performance of the conventional QRM-MLBD with CP insertion is also plotted for comparison. The training sequence (TS) aided QRM-MLBD with TS length of 16 symbols [9] is used similar to the conventional QRM-MLBD with CP insertion.

It can be seen from Fig. 4 that overlap QRM-MLBD improves the throughput performance when smaller number X of the symbols to be picked up is used. This is because at early stages of M-algorithm, the IBI from the next block is less significant. However, the use of smaller X increases the detection complexity. It can also be seen that the throughput is sufficiently improved by using iterative processing even if large X is used. With no iteration ($I=0$), $X=4$ should be used to sufficiently improve the throughput performance. However, when $I=1$, much larger X (e.g. $X=48$) can be used. Since iterative overlap QRM-MLBD does not require the CP insertion, the peak throughput is higher than that of the conventional QRM-MLBD with CP insertion.

B. Computational Complexity

In this paper, the computational complexity is defined as the number of real multiplications per symbol. Figure 5 plots the complexity as a function of N_c (corresponding to the size of the observation window) when the best combination of I and X to achieve a throughput of 8.0 bps/Hz with lowest complexity is used. When smaller N_c is used, larger I and smaller X are

needed to suppress the IBI sufficiently. Therefore, the complexity of the path metric computation increases. On the other hand, the size of the channel matrix is small and therefore, the complexity of the QR decomposition reduces. It is understood from Fig. 5 that the computational complexity to achieve a peak throughput of 8.0 bps/Hz is lowest when $N_c=28$ and is about 60% of the conventional QRM-MLBD ($N_c=64$) with CP insertion.

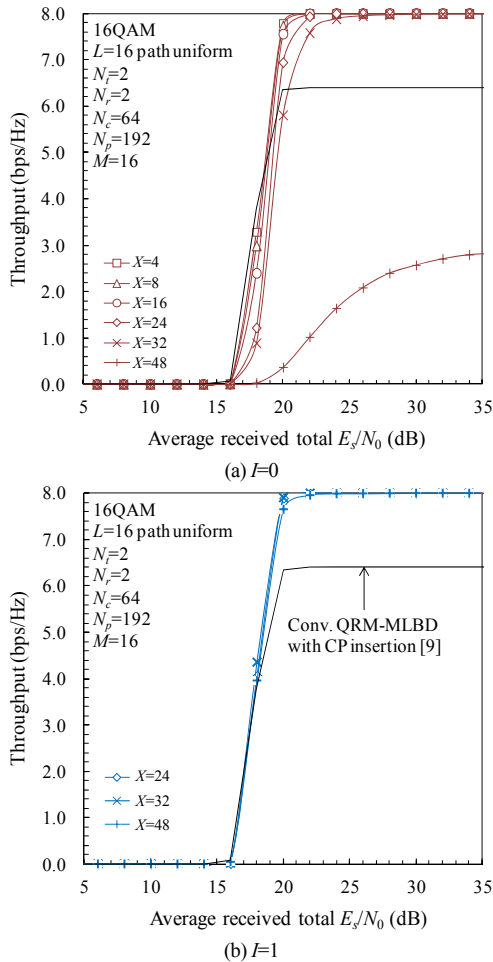


Figure 4. Throughput performance.

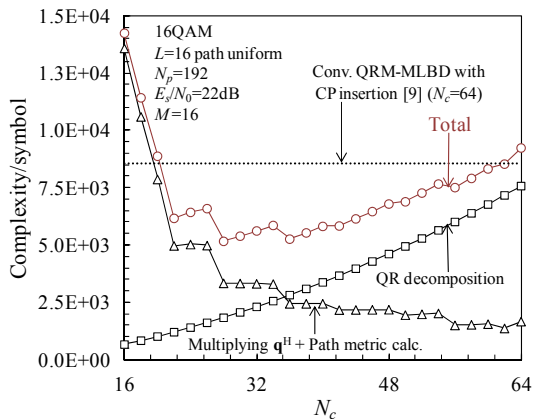


Figure 5. Impact of N_c on complexity.

IV. CONCLUSION

In this paper, we proposed an overlap QRM-MLBD which requires no CP insertion for the SC-MIMO spatial multiplexing. Remembering that the IBI exists near the bottom of the elements in the overall received signal vector for QRM-MLBD in SC-MIMO, only the reliable symbols are picked up after performing QRM-MLBD. To detect a continuously transmitted symbol stream, the present observation window for performing QRM-MLBD is overlapped with previous and next observation windows. To further improve the detection performance, iterative processing was introduced. We showed that the proposed overlap QRM-MLBD improves the throughput by 125% than the conventional QRM-MLBD with CP insertion ($N_c=64$, $N_g=16$). The computational complexity can be reduced to 60% of the conventional QRM-MLBD with CP insertion ($N_c=64$).

REFERENCES

- [1] G. J. Foschini and M. J. Gans, "On limits of wireless communications in a fading environment when using multiple antennas," *Wireless Personal Commun.*, Vol. 6, No. 3, pp. 311-335, 1998.
- [2] H. Ekstrom, A. Furuskar, J. Karlsson, M. Meyer, S. Parkvall, J. Torsner, and M. Wahlqvist, "Technical solutions for the 3G long-term evolution," *IEEE Commun. Mag.*, Vol. 44, No. 3, pp. 38-45, Mar. 2006.
- [3] N. Benjamin, L. Chan-Tong, and D. Falconer, "Turbo frequency domain equalization for single-carrier broadband wireless systems," *IEEE Trans. Wireless Commun.*, Vol. 6, No. 2, pp. 759-767, Feb. 2007.
- [4] K. Higuchi, H. Kawai, N. Maeda, H. Taoka, and M. Sawahashi, "Experiments on real-time 1-Gb/s packet transmission using MLD-based signal detection in MIMO-OFDM broadband radio access," *IEEE Journal on Selected Areas in Commun.*, Vol. 24, No. 6, pp. 1141-1153, June 2006.
- [5] 3GPP, PR-050758, "LS on UTRAN LTE multiple access selection," Nov. 2005.
- [6] J. G. Proakis and M. Salehi, *Digital communications*, 5th ed., McGraw-Hill, 2008.
- [7] A. Nakajima, D. Garg, and F. Adachi, "Throughput of turbo coded hybrid ARQ using single-carrier MIMO multiplexing," *Proc. IEEE 61st Vehicular Technology Conference (VTC2005-Spring)*, Vol. 1, pp. 610-614, 30 May-1 June 2005.
- [8] K. Nagatomi, K. Higuchi, and H. Kawai, "Complexity reduced MLD based on QR decomposition in OFDM MIMO multiplexing with frequency domain spreading and code multiplexing," *Proc. IEEE Wireless Communications and Networking Conference (WCNC 2009)*, Apr. 2009.
- [9] T. Yamamoto, K. Takeda, and F. Adachi, "Training sequence-aided QRM-MLD block signal detection for single-carrier MIMO spatial multiplexing," *Proc. IEEE International Conference on Communications (ICC 2011)*, June 2011.
- [10] I. Martoyo, T. Weiss, F. Capar, and F. K. Jondral, "Low complexity CDMA downlink receiver based on frequency domain equalization," *Proc. IEEE 58th Vehicular Technology Conference (VTC) Sept. 2003*.
- [11] T. Obara, K. Takeda, K. Lee, and F. Adachi, "Performance comparison of overlap FDE and sliding-window chip equalization for multi-code DS-SS-CDMA in a frequency-selective fading channel," *IEICE Trans. Commun.*, Vol. E94-B, No.3, pp.750-757, Mar. 2011.
- [12] K. Ishihara, Y. Takatori, S. Kubota, and F. Adachi, "Multiuser detection for asynchronous broadband single-carrier transmission systems," *IEEE Trans. Vehicular Technology*, Vol. 58, No. 6, pp. 3055-3071, July 2009.
- [13] H. Moroga, T. Yamamoto, and F. Adachi, "Overlap QRM-ML block signal detection for single-carrier transmission without CP insertion," *Proc. IEEE 75th Vehicular Technology Conference (VTC2012-Spring)*, May 2012.
- [14] H. Moroga, T. Yamamoto, and F. Adachi, "Iterative overlap TD-QRM-ML block signal detection for single-carrier transmission without CP insertion," *Proc. IEEE 78th Vehicular Technology Conference (VTC2012-Fall)*, Sept. 2012.
- [15] J. B. Anderson and S. Mohan, "Sequential coding algorithms: A survey and cost analysis," *IEEE Trans. Commun.*, vol. 32, pp. 169-176, Feb. 1984.